Sensors & Actuators: B. Chemical 359 (2022) 131547

Contents lists available at ScienceDirect

Sensors and Actuators: B. Chemical

journal homepage: www.elsevier.com/locate/snb

# Bioinspired bilayer hydrogel-based actuator with rapidly bidirectional actuation, programmable deformation and devisable functionality

Weizhong Xu [a], Pengli Dong [a], Senpeng Lin [b], Zhongwen Kuang [a], Zhiqin Zhang [a], Shunli Wang [a], Fangmin Ye [a], Lin Cheng [a], Huaping Wu [b,*], Aiping Liu [a,*]

[a] Key Laboratory of Optical Field Manipulation of Zhejiang Province, Faculty of Mechanical Engineering & Automation, Zhejiang Sci-Tech University, Hangzhou 310018, PR China

[b] Key Laboratory of Special Purpose Equipment and Advanced Processing Technology, Ministry of Education and Zhejiang Province, College of Mechanical Engineering, Zhejiang University of Technology, Hangzhou 310023, PR China

ARTICLE INFO

*Keywords:*
Bilayer structure
Hydrogel-based actuator
Airlaid paper
Bidirectional actuation
Programmable deformation

ABSTRACT

Smart hydrogel actuators which respond to external stimuli have attracted great attention and shown good application prospects in many fields as their simplicity and reliability, while the challenges remain in terms of the relatively low driving force, responsive velocity and deformation amplitude considering the structure-dependent actuation behavior. Here, we propose a thermosensitive hydrogel-based actuator with bioinspired bilayer structure by applying a textured airlaid paper to induce the formation of heterogeneous construction. This nature-inspired design benefits the hydrogel-based actuator rapidly bidirectional actuation, realizing excellent bending velocity (140.6° $s^{-1}$ within first 5 s) and bending amplitude (850.0° within 30 s) in hot water, powerful recovery in cool water and remarkable reproducibility upon external environmental stimulus by optimizing the texture orientation and mechanical property of airlaid paper. The excellent bonding between airlaid paper and hydrogel also endows the actuator satisfactory stability for circularly operation under water environment for weeks. The programmable deformation and devisable functionality are further realized by propagable and elaborate design for architecture and component of responsive hydrogel, favoring the hydrogel-based actuator alterable ethanol-sensitive ability, photothermal drivability and regenerability. This bilayer hydrogel-based actuator provides promising potentials for the applications in soft robots, smart actuators, artificial muscles, and intelligent human-machine technologies.

## 1. Introduction

The development of soft actuators is an important area of research considering their three-dimensional controllable and programmable shape transformation upon the trigger of specific external environmental stimuli [1–4], such as pressure [5,6], temperature [7–9], light [10,11], pH [12,13], ions [14,15], solvent [16,17], electric and magnetic fields [18–20]. As one of the most typical and outstanding representatives, hydrogel actuator can enable the development of manipulators or grippers [6,7], microfluidic valves [21,22], drug delivery systems [23], tissue engineering [24,25], active optical lenses [26], multifunctional sensors [27,28] and artificial muscles [29]. The stimuli-responsive properties of hydrogels are a prerequisite for hydrogel actuators, however, homogeneous hydrogels usually only achieve macroscopic expansion/contraction by swelling/deswelling under homogeneous stimulus, which restricts their further application. A promising approach in this respect is to replace in-plane deformation with out-of-plane deformation (bending/unbending) by constructing the inhomogeneous structure of hydrogel. Until now, a variety of anisotropic structures, including bilayer structures [7,8,12,13,30,31], gradient structures [22,32], patterned structures [33,34], oriented structures [17,35,36] and some others [37,38] have been designed and fabricated. Among these, bilayer structures are particularly attractive because of their flexible and diversified design in the two-layer hydrogels with structure and performance difference [12,13,30,31]. However, the delamination at the interface after multiple deformation is still major limit for their long-term engineering applications, and the challenges remain in terms of the relatively low driving force, responsive velocity and deformation amplitude of hydrogel actuators.

Nature is always a perpetual source of inspiration for scientists to

* Corresponding authors.
*E-mail addresses:* wuhuaping@gmail.com, hpwu@zjut.edu.cn (H. Wu), liuaiping1979@gmail.com, liuap@zstu.edu.cn (A. Liu).

https://doi.org/10.1016/j.snb.2022.131547
Received 26 November 2021; Received in revised form 2 February 2022; Accepted 5 February 2022
Available online 10 February 2022

research hydrogel actuators. The biomimetic actuating systems based on natural systems such as inchworm [39], fish [40], chameleon [41], Mimosa [42], Venus flytrap [43] and sunflower [44] have been proposed to promote the performances of hydrogel actuators. In addition, as one type of carnivorous waterwheel plant, the Aldrovanda vesiculosa is tenfold faster than Venus flytrap at snap-traps, and its underwater traps can shut within approximately 20–100 ms. This super-fast motion is mainly due to its unique layered and striated motor zones (Fig. 1a1-a3), allowing the outer epidermal cell layers to bend due to the rapid loss of turgor at inner epidermal cells upon triggering by action potentials [45–47]. Inspired by the layered structure of motor zones of Aldrovanda vesculosa, we herein present a hydrogel-based actuator with similar bilayer structure, namely a thermosensitive Poly (N-isopropylacrylamide) (PNIPAM) hydrogel layer as the active layer and a striated thin airlaid paper as the textured passive layer. Compared to traditional fibrous paper, the airlaid paper, as one of nonwovens, is composed of cellulose fibers and polyester fibers, and has rough striped structure and excellent stability in water [48,49]. It can also be flexibly treated by different solutions, such as acerbic, alkaline, organic or polymer solvents to changes its mechanical property, which is greatly helpful for the construction of heterogeneous structure and the improvement of actuation behavior of hydrogel-based actuator in an aqueous environment. This thermo-responsive deformation of the bilayer hydrogel-based actuator can be realized when environment temperature is above and subsequently below the lower critical solution temperature (LCST) of PNIPAM hydrogel, resulting in the contraction and expansion of hydrogel network (Fig. 1b2-d2) and a fast, reversible, bidirectional bending/recovery action (Fig. 1b1-d1). Compared with the traditional double-layer hydrogel structure, our design presents excellent actuation performance, typical bending velocity of 140.6° $s^{-1}$ within first 5 s and bending amplitude of 850.0° in hot water, powerful recovering to the initial state within 2 min in cool water, and reversed bending to the maximum bending amplitude of 1377.1° within 5 min. Meanwhile, a series of controllable and programmable deformations are realized by well-designed patterned architectures. The universality for constructing the bilayer hydrogel-based actuator is verified by changing the component and type of responsive hydrogel or physical property of passive layer, favoring the actuator alterable ethanol-sensitive ability, photothermal drivability and regenerability.

## 2. Material and methods

### 2.1. Materials

N-isoproplacrylamide (NIPAM) monomer, purified by tertiary recrystallization, was purchased from Shanghai Aladdin Chemical Agent

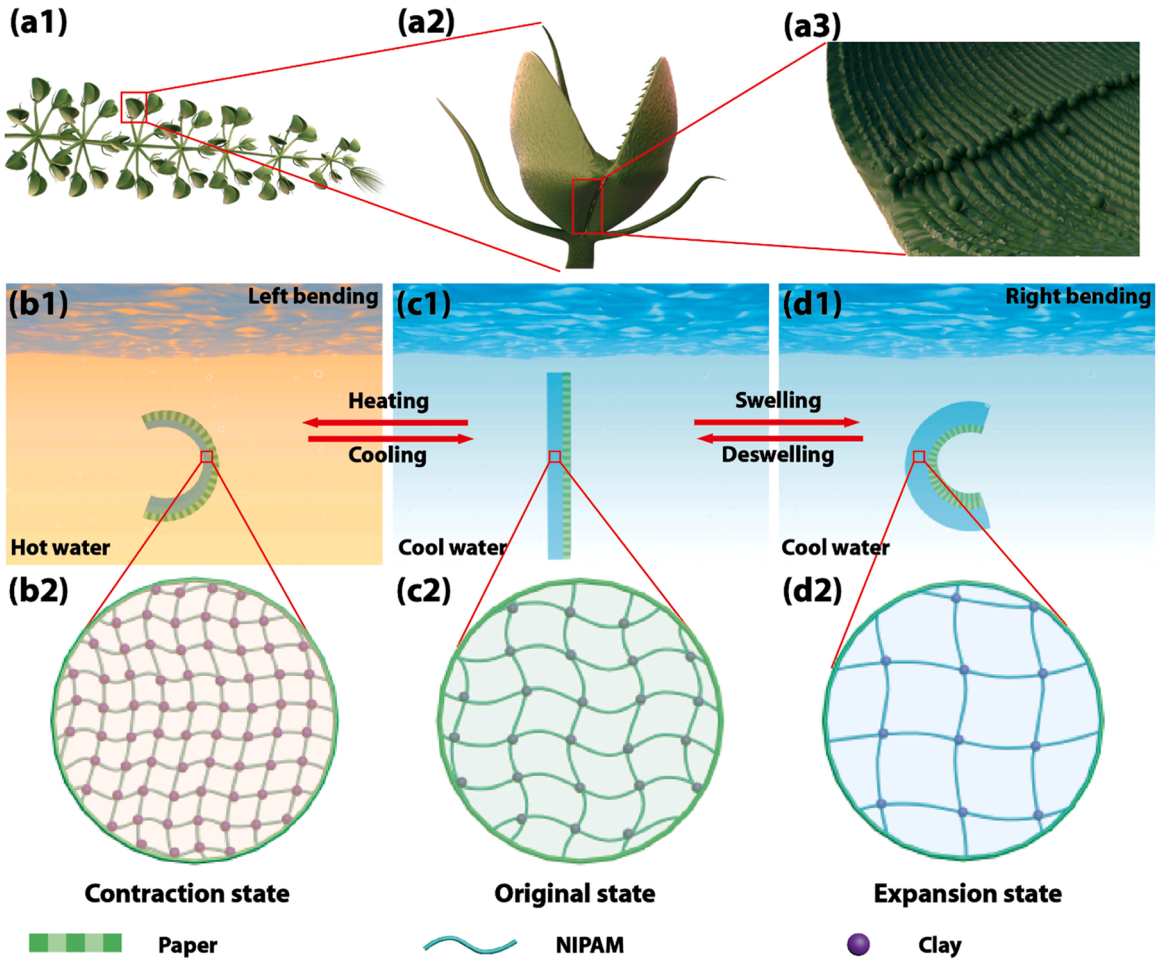


**Fig. 1.** Schematic illustration of the thermo-responsive deformation mechanism of the bilayer hydrogel-based actuator. (a1-a3) Schematic illustration of the morphology of Aldrovanda vesiculosa at different parts including (a1) overall view, (a2) an opening trap, and (a3) striated motor zones. (b1-d2) Schematic representation of the actuation behavior and corresponding hydrogel network of bioinspired bilayer hydrogel-based actuator in (b1, b2) contraction state, (c1, c2) original state, and (d1, d2) expansion state. The PNIPAM hydrogel presents a volume contraction after dehydration when the external ambient temperature is higher than the LCST of PNIPAM, resulting in the actuator bends toward the hydrogel side in hot water (b1,b2). Conversely, when the environment temperature is below the LCST of PNIPAM, the contracted hydrogel network would generate swelling, recovering and even expansion exceeding its original volume, resulting in actuator recovering (c1,c2) and reverse bending toward paper side in cool water (d1,d2). This bending-recovery process is reversible.

Co., Ltd (China). The synthetic hectorite "Laponite XLG" ($[Mg_{5.34}Li_{0.66}Si_8O_{20}(OH)_4]Na_{0.66}$) was purchased from Rockwood Chemicals Co., Ltd (China), and used as the inorganic clay after drying at 130 ℃ overnight. Acrylamide (AAM), N-N′-methylenebis(acrylamide) (MBAA), 1-Hydroxycyclohexyl phenyl ketone (Irg. 184), 2–2′-azo-bis-(2-methylpropionamidine) (V-50), 2-acrylamido-2-methylpropanesulfonic acid (AMPS), methanol, hydrochloric acid (HCl), N-methyl-2-pyrrolidone (NMP), ethanol, Poly(vinyl alcohol) (PVA 1788), Chitosan (CS, low viscosity, < 200 mPa s), Glutaraldehyde, carbonnanotube (CNT) and Sodium hydroxide (NaOH) were purchased from Shanghai Aladdin Chemical Agent Co., Ltd (China). Airlaid paper, stored at 60 ℃, was purchased from Suzhou TaiNuo Purification Co., Ltd (China). All other chemicals used in this work were commercially available and analytical pure, and were used without any further purification. Deionized water (18.25 MΩ cm at 25 ℃) from a ultra-pure water system (Shanghai GaoSen Instrument Equipment Co., Ltd) was used throughout the experiments.

### 2.2. Preparation of PNIPAM-clay nanocomposite hydrogel

The synthetic procedure for PNIPAM-clay (NC) nanocomposite hydrogel was the same as that reported previously [7]. Typically, uniform aqueous solution containing NIPAM monomer, crosslinker (Laponite XLG), and photoinitiator (Irg. 184) was prepared. The crosslinker (Laponite XLG, 10–100 mmol $L^{-1}$) was first dispersed in water and stirred for 4 h. Then, the NIPAM monomer (1.0 mol $L^{-1}$) was added into the clay suspension and stirred in an ice-water bath for another 2 h. Subsequently, photoinitiator solution (2.26 mg Irg. 184 was dissolved in 100 μL methanol) was added into former solution in ice-water bath with stirring. The concentration ratio of photoinitiator to monomer was fixed at 0.2 wt%. Throughout all experiments, oxygen was excluded from the system by a continuous infusion of nitrogen. Then, the precursor solution was injected into the molds (40 mm × 10 mm in length × width) with two transparent quartz glass plates and a silicon rubber spacer with a specific shape. Finally, the system was exposed to the ultraviolet irradiation (365 nm, 250 W) for 3 min in ice-water bath to obtain the NC hydrogel after peeling off the mold. A series of PNIPAM hydrogels with different clay proportions were prepared by changing the clay concentration from $1 \times 10^{-2}$ mol $L^{-1}$ to $10 \times 10^{-2}$ mol $L^{-1}$ and the corresponding samples were defined as NC$x$ ($x = 1, 3, 5, 7, 10$) hydrogels.

### 2.3. Preparation of P(AAm-co-AMPS) hydrogel

AAm (0.887 g, monomers), AMPS (0.180 g, monomers), MBAA (0.035 g, a chemical cross-linker), V-50 (0.045 g, a photoinitiator) were dissolved in 8.86 mL deionized water and stirred to obtain a homogenous solution. Then, the precursor solution was transfused into a reaction cell composed of two transparent quartz glass plates and a silicon rubber spacer. After UV irradiation (365 nm, 250 W) for 4 min, the P(AAm-co-AMPS) hydrogel was obtained.

### 2.4. Modification of airlaid paper and leaf

The airlaid paper was physically or chemically modified by soaking it in different liquids overnight, and then dried under vacuum at 50 ℃. The modified liquids included 1 mol $L^{-1}$ HCl, NMP, ethanol, PVA solution, CS solution and CNT-including suspension. The PVA solution (10 mg $mL^{-1}$) was prepared by dissolving PVA powder in deionized water at 60 ℃. The CS solution (10 mg $mL^{-1}$) was formed by dissolving CS powder in 1% acetic acid and deionized water. The CNT-including suspension (5 mg $mL^{-1}$) was produced by dispersing CNT and surfactant sodium dodecyl sulfate (SDS, 1:2 wt%) in deionized water and sonicating for 30 min. The modified papers were successively called as "Paper-HCl", "Paper-NMP", "Paper-ethanol", "Paper-PVA", "Paper-CS", and "Paper-CNT" and cut into specific sizes before use. Note that both "Paper-PVA" and "Paper-CS" were cross-linked by soaking in 1% glutaraldehyde solution for 24 h. The air-dried maple leaf was rinsed with deionized water. The fresh camphor leaf was picked and washed, then transferred into 10% NaOH solution and boiled for 10 min. Afterwards, a soft bristle brush was used to remove excess flesh, leaving a complete vein skeleton. All modified leaves were pressed at 60 ℃ for 30 min to form films.

### 2.5. Preparation of bilayer hydrogel-based actuator

The airlaid paper with suitable dimensions (40 mm × 10 mm in length × width) and silicon rubber spacer with variable thickness were successively placed on the glass plate. The precursor solution mentioned above was injected into the mold with another glass plate to seal the vessel. Then the bilayer hydrogel-based actuator was prepared after in-situ polymerization under UV irradiation (365 nm, 250 W) (Fig. 2a1-a4).

### 2.6. Characterization

The surface and cross section morphologies of the samples were observed by a field-emission scanning electron microscopy (SEM, S-4800, Hitachi, Tokyo, Japan) at an acceleration voltage of 3 kV. Before the measurement, the samples were frozen in liquid nitrogen and then freeze-dried for more than 24 h at − 80 ℃ with a freeze-dryer (Shanghai Leewen Scietific Instrument Co., Ltd.). The volume phase transition temperature of the hydrogel was analyzed on a differential scanning calorimeter (DSC, TA DSC Q200, USA) by heating the hydrogel from 25 ℃ to 50 ℃ at a scanning rate of 5 ℃ $min^{-1}$ under nitrogen. For the tensile mechanical properties of the papers and hydrogels, the samples were cut into a test rectangular shape (40 mm in length, 10 mm in width), and were evaluated by using the mechanical testing machine (Instron 5943, USA) at a displacement rate of 10 mm $min^{-1}$. The Young's modulus of samples was obtained by calculating the slope of the stress-strain curve at strain of 0–5%. In order to evaluate the binding force between airlaid paper and hydrogel, the samples were fixed to the glass sheet for interface peel test by using the mechanical testing machine at a rate of 10 mm $min^{-1}$. At least five samples were tested for each experimental condition to obtain statistically reliable values.

In order to evaluate the actuation behaviors of the bilayer hydrogel-based actuators, two glass jars loaded with deionized water were heated to 20 ℃ (cool water) and 50 ℃ (hot water), respectively. The hydrogels were all cut into strips of 40 mm in length and 10 mm in width, one end of the long axis of the hydrogel was secured with a clamps, and the other end was in free suspension. Subsequently, the hydrogel strip was immersed vertically in hot water, and the strip bended quickly toward the hydrogel side in response to the high temperature. Once the maximum bending angle was reached, the strip was transferred to cool water again to recover and even bend in the other direction. The whole dynamic process was recorded with a digital camera to determine the bending angle of hydrogel by the screenshot at different time points. The bending angle-time relations were acquired by analyzing print screens with Image J software. The bending angle was determined by the deformation central angle as reported in previous research (Fig. S1) [8,22,32,44]. The bending amplitude was defined as the difference between the maximum bending angle and the initial bending angle. Bending velocity was calculated according to the bending angle in the corresponding time period. The bending-recovery test was repeated 20 times to demonstrate the cycle performance. The above procedure was repeated five times for each sample to evaluate the reliability of the results.

### 2.7. Finite-element analysis

The finite element analyses were performed to reveal the stress distribution and demonstrate the swelling mechanism of the multiple patterned bilayer hydrogel-based actuators. An explicit model was

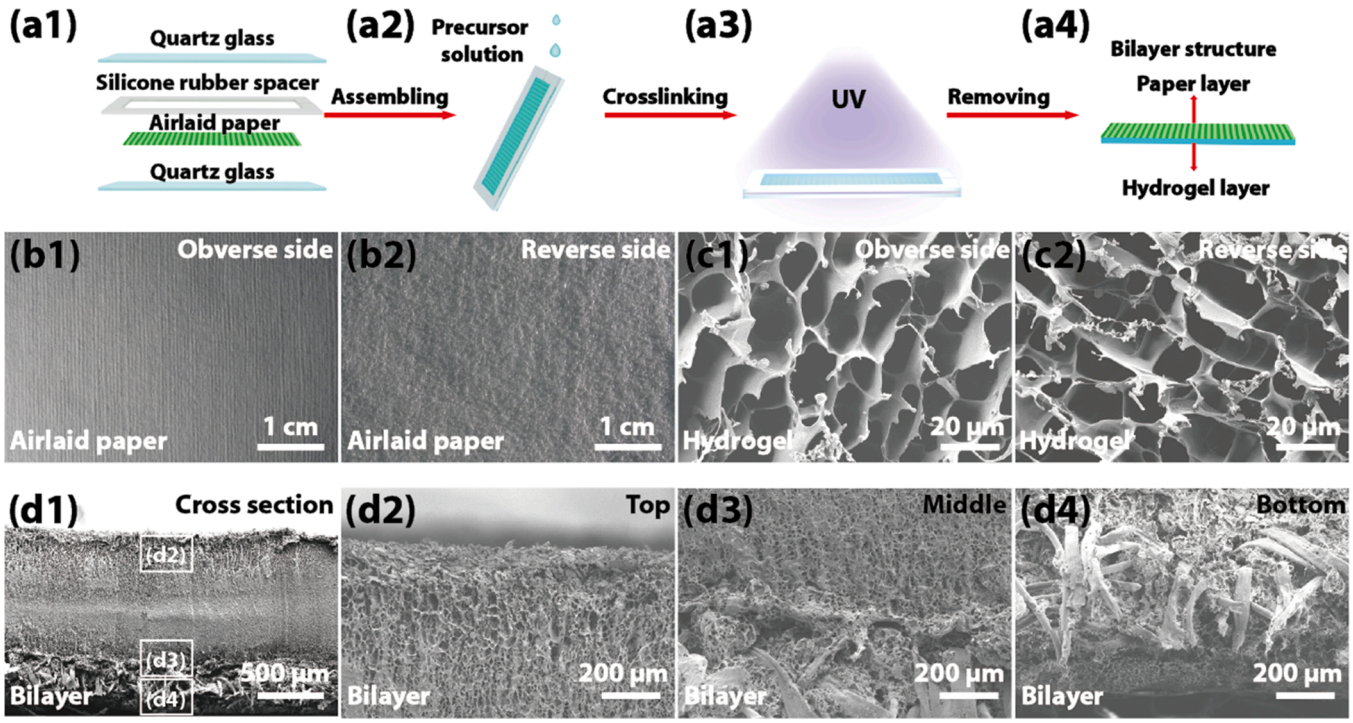


**Fig. 2.** Preparation and morphology characterization of the bilayer hydrogel-based actuator. (a) Schematic illustration of the fabrication process of the bilayer hydrogel-based actuator; SEM images of (b1) obverse side and (b2) reverse side of airlaid paper; SEM images of (c1) obverse side and (c2) reverse side of PNIPAM hydrogel; SEM images of cross section of bilayer structure at different locations including (d1) overall view, (d2) top layer, (d3) middle interface, and (d4) bottom layer.

constructed in commercial package ABAQUS 6.14. The solid elements C3D8H were employed to characterize the three-dimensional hydrogel structure. The temperature shift was applied to the bilayer hydrogel-based actuators with different patterns, such as texture orientation of airlaid paper layer, the specific deformation of capital letters ("ZSTU"), and different grippers, to reveal the stress distribution.

## 3. Results and discussion

### 3.1. Microstructure of the thermosensitive bilayer hydrogel-based actuator

The porous airlaid paper is composed of cellulose fibers and polyester fibers and has a thickness of about 250 μm. The optical and SEM images obviously show the rough cellulose fiber bundles with striped structure at the obverse side of airlaid paper (Fig. 2b1; Fig. S2a,b, Supporting information) and smooth polyester fibers with random distribution at the reverse side of airlaid paper (Fig. 2b2; Fig. S2c,d). According to the bioinspired synergism, the contact between the reverse side of airlaid paper (polyester fibers) and hydrogel is not only conducive to their close combination with each other, but also facilitates the actuation behavior by exposing the striated structure at the obverse side of the airlaid paper (cellulose fibers). From the SEM images of pure PNIPAM hydrogel without airlaid paper, the gel exhibits isotropic porous microstructure with the pore diameter about 20 μm (Fig. 2c1-c2). While the hydrogel-paper bilayer presents an interpenetrating interface due to the interconnection between the paper fibers and the hydrogel network (Fig. 2d1-d4) with the thickness ratio of the paper layer to the hydrogel one about 1:4 (Fig. 2d1, $h_{paper}/h_{hydrogel} = 1{:}4$, the thickness of the hydrogel layer is about 1000 μm).

### 3.2. Temperature-responsive actuation behavior of bilayer hydrogel-based actuators

#### 3.2.1. Effect of hydrogel layer on actuating performance

PNIPAM hydrogel as a well-known thermal-responsive polymer has obvious changes in volume and pore diameter before and after the phase transition due to the volume contraction after dehydration when the external ambient temperature is higher than the LCST of the active layer (Fig. S3). While the passive layer retains unchanged, resulting in the actuator bends toward the hydrogel side in hot water (Fig. 1b1). Conversely, when the environment temperature is below the LCST of the active layer, the contracted hydrogel network would generate swelling, recovering and even expansion exceeding its original volume, resulting in actuator recovering and reverse bending toward paper side in cool water (Fig. 1c1,d1) [50,51]. Therefore, the anisotropic actuation motion is primarily induced by the large mismatch in volume change and stress of these two layers. The actuating performance of the bilayer hydrogel-based actuator under temperature stimulus was evaluated by measuring the bending angle-time relations and bending velocity in water (Fig. S1). Here, we define an effective actuation force ($F_{eaf}$) to evaluate the actuation performance [7,42,52,53], the larger this value, the better actuation performance. This $F_{eaf}$ can be described through a simple equation

$$F_{eaf} = F_{haf} - F_{hr} + F_{paf} - F_{pr} \quad (1)$$

where $F_{haf}$ is the actuation force caused by temperature responsive volume contraction/expansion of hydrogel layer, $F_{hr}$ is the resistance of hydrogel layer, including its own gravity, pressure of water, internal stress, etc. $F_{paf}$ is the actuation force of paper layer, which can be ignored because of the insensitive to temperature for paper layer. $F_{pr}$ is the resistance of paper layer. According to this equation, we can qualitatively evaluate the actuation performance of bilayer hydrogel-based actuator.

As a typical bilayer structure, the component and relative thickness

of hydrogel layer and texture orientation and mechanical property of the paper layer will influence the actuating performance of bilayer hydrogel-based actuator. Herein, a series of PNIPAM hydrogels with different clay proportions (NC$x$, $x$ = 1, 3, 5, 7, 10) were first prepared. The DSC results show that with the increase of clay concentrations in the range of 10–100 mmol $L^{-1}$, the LCST of NC hydrogel increases gradually form 31.8 to 33.3 ℃ (Fig. S4) and the thermos-responsive volume-changing rate will decrease [7,54]. This could be attributed to the restricted coil-to-globule phase transformation of NIPAM chains by steric hindrance of clay platelets at sufficiently high clay concentrations [54,55]. The clay concentration in the reaction system greatly influence the actuation behavior of bilayer structure at a given $h_{paper}/h_{hydrogel}$ of 1:4. The bilayer NC1 hydrogel-based actuator demonstrates a bending deformation towards hydrogel side under the generated $F_{haf}$ due to the volume shrinking of hydrogel in the 50 ℃ hot water and gradually reverts to its original state in the 20 ℃ cool water (Fig. S5a,b). The bilayer NC3 hydrogel-based actuator presents a quicker bending deformation to 123.7° in the first 5 s and to 608.6° at 30 s in the hot water, and quick recovery in the cool water within 2 min (Fig. 3a1). The bending velocity and maximum bending angle decrease with the further increase of clay concentration in the reaction system (Fig. S5c,d), until the mechanical force caused by the conformational change in NC10 hydrogel is too little to support regular bending. Theoretically, the $F_{hr}$ and $F_{pr}$ basically remain constant, while the $F_{haf}$ decreases with the increase of clay concentration, resulting in the gradual decrease of $F_{eaf}$ and the reducing of actuation performance of bilayer hydrogel-based actuator. Noteworthily, the tight connection between the paper layer and the PNIPAM hydrogel one is verified by the interface peel test. During the peeling process, no interface delamination is observed until the hydrogel layer was broken (Fig. S6), indicating the strong combination between PNIPAM hydrogel and paper layer.

In addition, the relative thickness of the paper layer and the hydrogel layer also greatly affects the actuating performance of the bilayer hydrogel-based actuator (Fig. S7). It should be noticed that the isotropous monolayer hydrogel without airlaid paper ($h_{paper}/h_{hydrogel}$ = 0:4) shows only volume contraction/expansion without obvious bending behavior in cool water or hot water. With the $h_{paper}/h_{hydrogel}$ increasing form 1:3 to 1:7, the actuating performance increases first and then decreases, with the maximum bending velocity in the first 5 s and bending amplitude for the first 30 s obtained in the bilayer system with $h_{paper}/h_{hydrogel}$ = 1:3. Since the $h_{paper}/h_{hydrogel}$ affects both $F_{haf}$ and $F_{hr}$, the actuating performance will be decreased due to the reduced external output force for the bilayer system with greater $h_{paper}/h_{hydrogel}$ [8,56]. The finite element simulation vividly shows the programmed bending

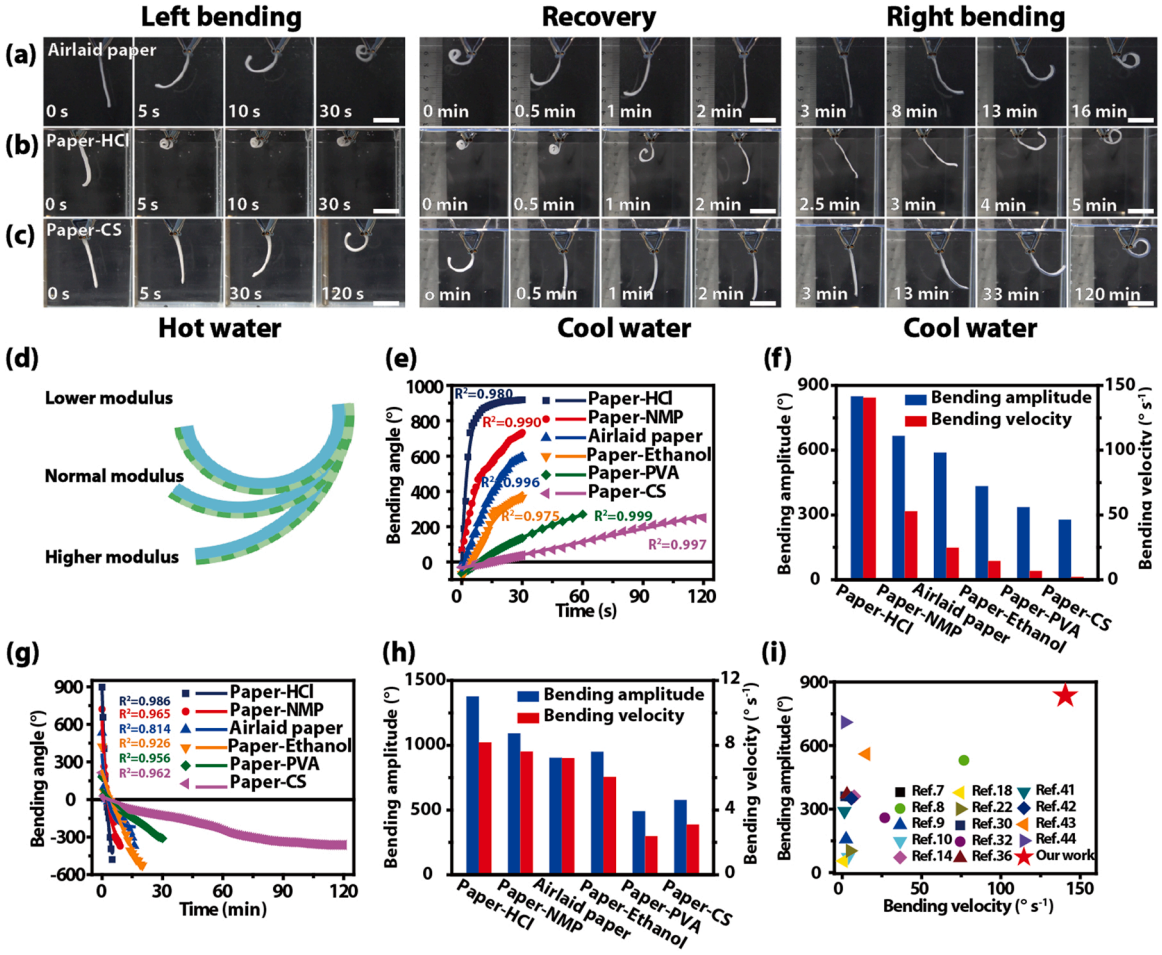


**Fig. 3.** Effect of mechanical property of paper layer treated by different solution on actuation performance of bilayer hydrogel-based actuators. (a-c) Optical photographs of bidirectional deformation process of bilayer hydrogel-based actuators with different mechanical property of paper layer. The bilayer strip was immersed vertically in hot water or cool water with the hydrogel side towards left (Scale bars were 1 cm.) (d) Schematic illustration of paper modulus related bending mechanism of the bilayer hydrogel-based actuators. The paper layer with lower modulus would reduce the resistance of actuator during deformation, resulting in faster bending rate and greater bending angle, vice versa. The relationship between the bending angle and time of different actuators in (e) hot water or (g) cool water, respectively. The overall bending amplitude and the initial bending velocity during the first 5 s or 60 s of different actuators in (f) hot water or (h) cool water, respectively. (i) Comparison of bending amplitude and bending velocity between our bilayer hydrogel-based actuator and other hydrogel-based actuators. All bilayer structures were prepared with NC3 hydrogels at a given $h_{paper}/h_{hydrogel}$ of 1:4.

process of bilayer hydrogel-based actuators with different stages (Fig. S8). These results indicate that the specifically actuating performance of bioinspired bilayer hydrogel-based actuator can be precisely adjustable by intentionally optimize the experiment parameters for broadly potential applications in certain situations.

### 3.2.2. *Effect of airlaid paper layer on actuating performance*

Commercial airlaid paper has a certain orientation for rough cellulose fiber bundle (Fig. 2b1). Therefore, we first focus on the effect of texture orientation of airlaid paper on the actuating behavior of bilayer hydrogel-based actuator. We define the angle between the direction of fiber bundle arrangement and the direction of long axis of strip-shaped actuator as the orientation angle of paper. As shown in Fig. 4, the bilayer actuator with different orientation angles of paper (0°, 30°, 45°, 60°, and 90°) could be designed and exhibit multimodal deformation when exposed to hot water (Movie S1). The bilayer actuators with 0° and 90° orientation angles could produce bending deformation along the short and long axes (Fig. 4a1 and e1), respectively, while the bilayer actuators with 30°, 45° or 60° orientation angles can be twisted into a helix with the helix radius increasing with the orientation angle (Fig. 4b1-d1). In fact, different deformation models have the same deformation direction, that is, bending occurs in the direction perpendicular to the texture orientation of strip-shaped actuator under the temperature stimulation [14,57,58]. These deformations can be simulated and predicted by constructing a finite element modeling of the shape transformation (Movie S2). The calculated stress distribution during deformation for all actuators presents a nice consistency in the theoretical simulation and experimental results (Fig. 4a2-e2, a3-e3), confirming the accurately controllable structure and programmable deformation of bilayer hydrogel-based actuator. The experiment results and force analysis also confirm that the mechanical anisotropy is closely related to the deformation model. Under the condition of keeping other parameters consistent, the direction of $F_{eaf}$ determines the deformation direction and the deformation form. Our experiment results verify that the anisotropic fiber bundle structure of airlaid paper brings its distinctively mechanical anisotropy (Fig. S9a-c). With the increase of orientation angle of airlaid paper, the maximum stress and Young's modulus gradually decrease, while the corresponding strain increases. Meanwhile, the bilayer actuators formed by PNIPAM hydrogel and different orientated papers also have anisotropic mechanical property (Fig. S9d-f) except for the relatively unchanged maximum strain when compared to the pure airlaid paper. Therefore, when the hydrogel layer undergoes isotropic volume contraction and generate isotropic actuating forces under temperature stimulation, the bilayer actuators are more likely to deform along the direction perpendicular to the texture orientation of strip-shaped actuator, and result in various deformation forms just like bending helix because the paper layer provides less resistance in this direction (possible one order of magnitude lower). In short, the direction of the paper's texture determines the direction of actuator deformation.

In order to further improve the actuating performance, an effective strategy is to reduce the $F_{pr}$ in Eq. (1), namely change the mechanical properties of the paper layer in a specific method. Therefore, we adopted a series of physical or chemical treatments by soaking the airlaid paper in different liquids including ethanol, HCl, NMP, PVA, and CS solutions to adjust the mechanical property of airlaid paper. From the SEM images, we can see that the bundles of cellulose fibers gradually break down into smaller fibers after being treated with acid (Paper-HCl, Fig. S10c) or strong solvent (Paper-NMP, Fig. S10d). The fiber surfaces are also loaded with a layer of molecular film after being treated with polymer solution (Paper-PVA and Paper-CS, Fig. S10e,f). Moreover, the paper's thickness, areal density, the maximum stress and Young's modulus decrease for HCl and NMP treated samples, while the samples treated by polymer solution display an opposite rule (Fig. S11). In particular, the Young's modulus of Paper-HCl and Paper-CS are 2.14 ± 0.16 MPa and 17.84 ± 1.17 MPa, respectively, presenting a 50% reduction and 320% increase when compared to the untreated paper (4.28 ± 0.44 MPa). The changes in the mechanical property of paper layer greatly affect the actuating performance of bilayer hydrogel-based actuators. With the increase of Young's modulus of modified paper, the actuating performances of bilayer hydrogel-based actuators (NC3) decrease significantly (Fig. 3a-c; Fig. S12) because the paper layer with lower modulus will reduce the resistance of actuator during deformation, resulting in faster bending rate and greater bending angle (Fig. 3d). Of particular note is that the bilayer hydrogel-based actuator prepared

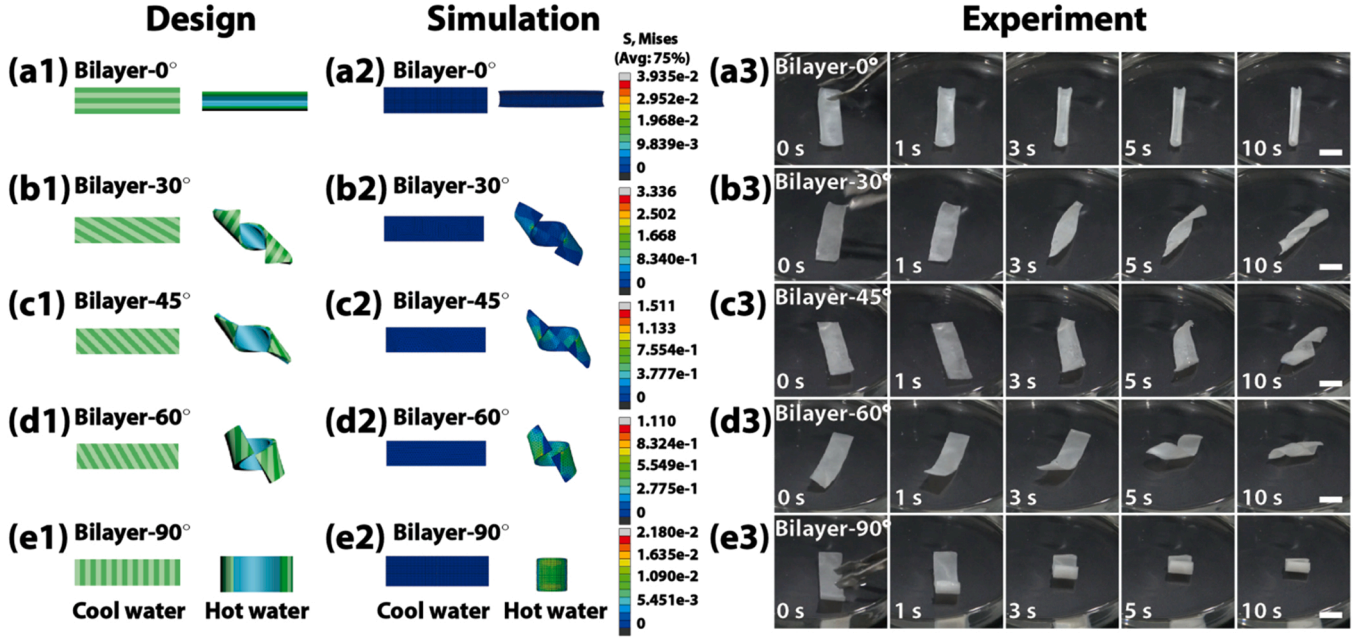


**Fig. 4.** Effect of texture orientation of airlaid paper layer on actuating performance. (a1-e1) Design of actuators, (a2-e2) simulation of stress distribution, and (a3-e3) experiment results demonstrate a nice consistency in the theoretical simulation and experimental results for multimodal deformation of bilayer hydrogel-based actuators with different orientation angles of airlaid paper layer including (a) 0°, (b) 30°, (c) 45°, (d) 60° and (e) 90° in hot water. All of the actuators were prepared by NC3 hydrogels with $h_{paper}/h_{hydrogel}$ = 1:4. Scale bars were 1 cm.

with HCl treated paper demonstrates unprecedented temperature-responsive deformation with an astonishing 703.2° bending within 5 s and 850.0° bending amplitude in 30 s in hot water, and 2-min recovery ability and reversed bending up to 1377.1° within 5 min when it is transferred to cold water (Fig. 3e-h; Movie S3). This bilayer hydrogel-based actuator exhibits excellent reversible and repeatable responsiveness, and could perform cycled deformation at least 20 times during heating and cooling processes without any noticeable loss of performance (Fig. S13). The optimized bilayer hydrogel-based actuator has more significant advantages in actuating performance, showing faster bending velocity (140.6° $s^{-1}$ in the first 5 s) and larger bending amplitude (850.0°) when compared to many reported temperature-responsive hydrogel-based actuators (Fig. 3i).

### 3.3. Applications and devisable functionality of bilayer hydrogel-based actuators

Based on the proposed bilayer structure, we design a series of pattern architectures to implement some special deformation. In order to realize this purpose, an airlaid paper with special design and geometry pattern was used for the construction of temperature-sensitive bilayer hydrogel-based actuators. Typically, four letter actuators with alterable geometry patterns and inhomogeneous structures are elaborately designed (Fig. S14). The well-designed actuators with local bilayer structures can perform the adjustable bending direction and bending amplitude via the local inhomogeneous volume shrinkage and stress distribution in order to realize the complexly controllable motion of soft actuators in hot water. In order to realize the bending of two ends of actuators towards completely opposite directions (such as "Z", "S" and "T"), the paper layer at joints are controlled to be opposite (Fig. S14). The theoretical simulation and experimental results agree well with each other, presenting the deformation of capital letters "ZSTU" (the English abbreviation of Zhejiang Sci-Tech University) in hot water (Fig. 5a-d; Movie S4 and Movie S5). Some temperature-controlled grippers with three arms, four arms and five arms are demonstrated from both practically and theoretically to accomplish petal-type closing and opening at an alternating hot and cold environment (Fig. S15). A wireless or wired capture and transportation of a tin foil paper ball can also be realized by a three-arm gripper with bilayer structure (Fig. S16).

To one's excitement, the universality and the effectiveness of the proposed method in constructing bioinspired bilayer structure as soft actuator is demonstrated by changing hydrogel layer or paper layer. First, the ethanol-sensitive P(AAm-co-AMPS) hydrogel was used as a substitute of thermosensitive PNIPAM hydrogel to prepare bilayer hydrogel-based actuator, demonstrating bending deformation toward the hydrogel layer in the ethanol bath because of the ethanol-induced volume contraction, a quick recovery and reversed bending in a water bath (Fig. 5e; Fig. S17). By soaking the airlaid paper with CNT-including

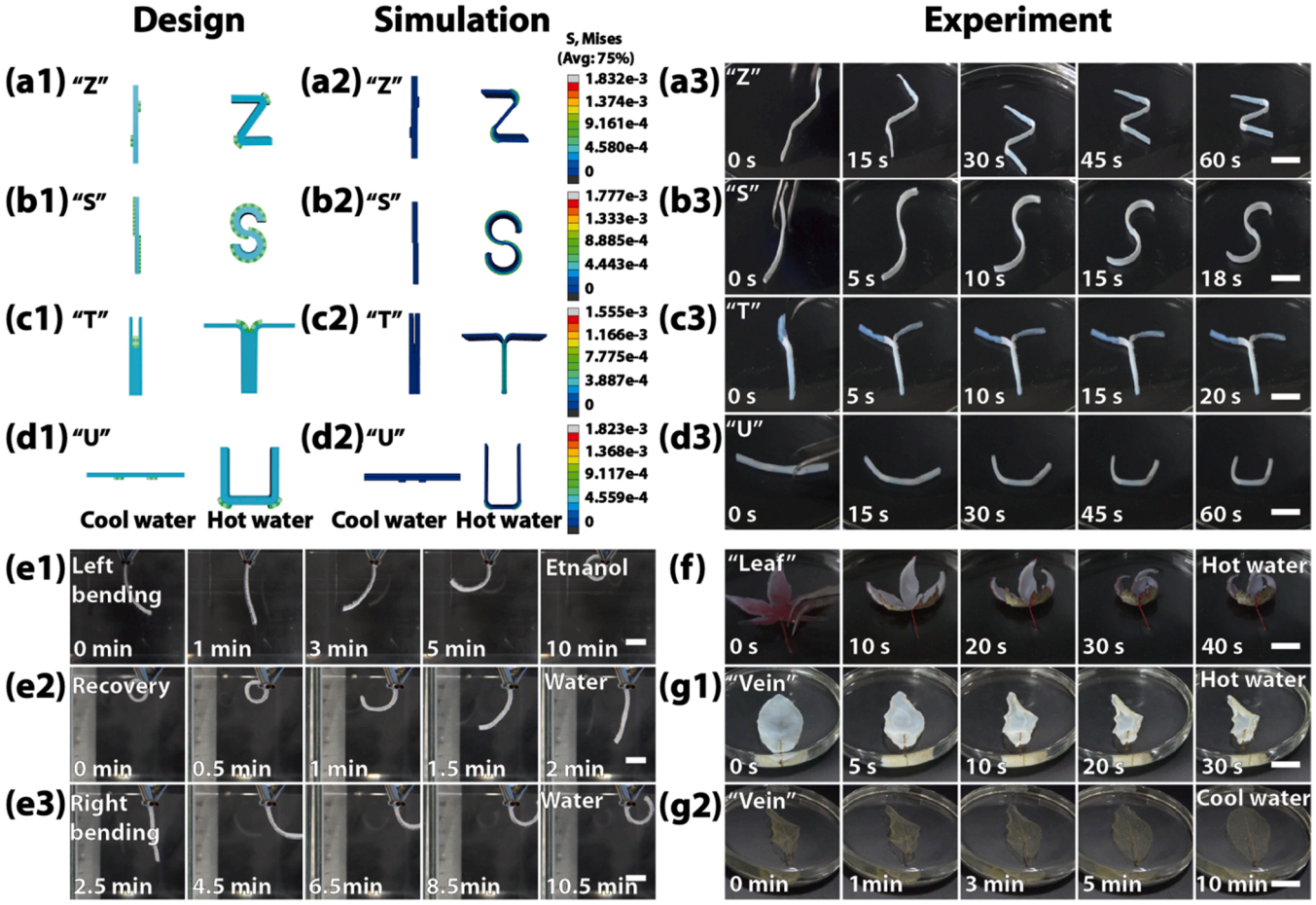


**Fig. 5.** Applications of bilayer hydrogel-based actuators and universality of the proposed method. (a1-d1) Design of actuators, (a2-d2) simulation of stress distribution, and (a3-d3) experiment results of bilayer hydrogel-based actuators, demonstrating programmable deformation in hot water. Actuators with different architectures carried out specific deformation of capital letters: (a) "Z", (b) "S", (c) "Z", and (d) "U" in hot water ("ZSTU" is the abbreviation of Zhejiang Sci-Tech University). (e-g) The universality of the proposed method was demonstrated by changing (e) hydrogel layer or (f, g) paper layer. (e) The optical photographs showed that P(AAm-co-AMPS) hydrogel displayed the typical (e1) left bending (in ethanol), (e2) recovery (in water), and (e3) right bending (in water) deformation process. (f, g) The optical photographs showed that (f) maple leaf or (g) leaf vein skeleton was used to replace paper layer to realize the typical (f, g1) wither (in hot water) or (g2) bloom (in cool water) deformation process. Scale bars were 1 cm.

solution, the obtained bilayer actuator displays photothermal drivability in cool water under laser irradiation (Fig. S18). By replacing the airlaid paper by maple leaf or leaf vein skeleton, the bilayer actuator realizes the typical wither (in hot water) or bloom (in cool water) deformation (Fig. 5f,g; Movie S6). Based on this strategy, we can realize the personalized customization of actuating type and deformation mode, and even integrate sensor or controller to build multi-function actuator.

At last, the regenerability of bilayer hydrogel-based actuator was also researched by a process of air-drying and re-swelling [59]. When the air-dried bilayer structure touches the cool water again, it will re-swell to restore the original form and function in a short time (~65 s), gradually swell and right bend to the maximum angle (−339.0°) within 3.5 min, and then rapidly carry out the left bending in the hot water (~15 s) (Fig. S19). The reversible actuation process has been repeated at least for 20 cycles within 4 weeks, indicating its good stability (Fig. S20). This air-drying and re-swelling strategy significantly extends the service life of actuator at the expense of some actuation performance decrease.

## 4. Conclusion

Inspired by the fast underwater motion of snap-traps of the Aldrovanda vesiculosa, we reported a bilayer hydrogel-based actuator consisting of hydrogel layer and airlaid paper layer through a simple and effective in-situ polymerization. By optimizing the structure-related parameters of the bilayer actuator, such as the component and relative thickness of hydrogel layer, texture orientation and mechanical property of the paper layer, the bilayer hydrogel-based actuator presented multimodal deformation with impressive bending velocity (140.6° $s^{-1}$ within first 5 s) and bending amplitude (850.0° within 30 s) in hot water, and excellent recovery and bidirectional bending performance in cool water. Meanwhile, we designed and assembled a series of well-designed pattern architectures, and successfully carried out programmable deformation including “ZSTU” capital letters and different grippers by means of the combination of theoretical simulation and controllable experiment. Quite interestingly, we could take advantage of the universality of the proposed method in constructing bioinspired bilayer structure as soft actuator to achieve the personalized customization of actuating type and deformation mode by arbitrarily changing the hydrogel layer or the paper layer. Our proposed bilayer hydrogel-based actuators could provide design inspiration in the field of soft robot, hydrogel actuator, artificial muscles, flexible electrics, and intelligent human-machine technology.

## CRediT authorship contribution statement

**Weizhong Xu:** Methodology, Software, Data curation, Writing – original draft. **Pengli Dong:** Data curation, Software, Validation. **Senpeng Lin:** Software, Formal analysis, Investigation. **Zhongwen Kuang:** Software, Validation. **Zhiqin Zhang:** Software, Validation. **Shunli Wang:** Formal analysis, Investigation. **Fangmin Ye:** Formal analysis, Investigation. **Lin Cheng:** Formal analysis, Investigation. **Huaping Wu:** Investigation, Supervision. **Aiping Liu:** Supervision.

## Declaration of Competing Interest

The authors declare that they have no known competing financial interests or personal relationships that could have appeared to influence the work reported in this paper.

## Acknowledgements

This work was supported by the Zhejiang Outstanding Youth Fund of China (No. LR19E020004), the Youth Top-notch Talent Project of Zhejiang Ten Thousand Plan of China (No. ZJWR0308010), the National Natural Science Foundation of China (No. 11672269 and 11972323), the Zhejiang Provincial Natural Science Foundation of China (No. LR20A020002), the Fundamental Research Funds for the Provincial Universities of Zhejiang of China (No. RF-B2019004) and Excellent Dissertation Program from Zhejiang Sci-Tech University of China (No. 2019D10).

## Appendix A. Supporting information

Supplementary data associated with this article can be found in the online version at doi:10.1016/j.snb.2022.131547.

## References

[1] D. Rus, M.T. Tolley, Design, fabrication and control of soft robots, Nature 521 (2015) 467–475, https://doi.org/10.1038/nature14543.
[2] X. Le, W. Lu, J. Zhang, T. Chen, Recent progress in biomimetic anisotropic hydrogel actuators, Adv. Sci. 6 (2019) 1801584, https://doi.org/10.1002/advs.201801584.
[3] S. Li, H. Bai, R.F. Shepherd, H. Zhao, Bio-inspired design and additive manufacturing of soft materials, machines, robot, and haptic interfaces, Angew. Chem. Int. Ed. 58 (2019) 11182–11204, https://doi.org/10.1002/ange.201813402.
[4] M. Ilami, H. Bagheri, R. Ahmed, E.O. Skowronek, H. Marvi, Materials, actuators, and sensors for soft bioinspired robots, Adv. Mater. 19 (2020) 20203139, https://doi.org/10.1002/adma.202003139.
[5] M. Wehner, R.L. Truby, D.J. Fitzgerald, B. Mosadegh, G.M. Whitesides, J.A. Lewis, R.J. Wood, An integrated design and fabrication strategy for entirely softe, autonomous robots, Nature 536 (2016) 451–455, https://doi.org/10.1038/nature19100.
[6] H. Yuk, S. Lin, C. Ma, M. Takaffoli, N.X. Fang, X. Zhao, Hydraulic hydrogel actuators and robots optically and sonically camouflaged in water, Nat. Commun. 8 (2017) 14230, https://doi.org/10.1038/ncomms14230.
[7] C. Yao, Z. Liu, C. Yang, W. Wang, X.-J. Ju, R. Xie, L.-Y. Chu, Poly(N-isopropylacrylamide)-clay nanocomposite hydrogels with responsive bending property as temperature-controlled manipulators, Adv. Funct. Mater. 25 (2015) 2980–2991, https://doi.org/10.1002/adfm.201500420.
[8] H. Lin, S. Ma, B. Yu, X. Pei, M. Cai, Z. Zheng, F. Zhou, W. Liu, Simultaneous surface covalent bonding and radical polymerization for constructing robust soft actuators with fast underwater response, Chem. Mater. 31 (2019) 9504–9512, https://doi.org/10.1021/acs.chemmater.9b03670.
[9] K. Liu, Y. Zhang, H. Cao, H. Liu, Y. Geng, W. Yuan, J. Zhou, Z.L. Wu, G. Shan, Y. Bao, Q. Zhao, T. Xie, P. Pan, Programmable reversible shape transformation of hydrogels based on transient structural anisotropy, Adv. Mater. 32 (2020) 2001693, https://doi.org/10.1002/adma.202001693.
[10] C.L. Zheng, F. Jin, Y.Y. Zhao, M.L. Zheng, J. Liu, X.Z. Dong, Z. Xiong, Y.Z. Xia, X. M. Duan, Light-driven micron-scale 3D hydrogel actuator produced by two-photon polymerization microfabrication, Sens. Actuators B-Chem. 304 (2020), 127345, https://doi.org/10.1016/j.snb.2019.127345.
[11] L. Breuer, J. Pilas, E. Guthmann, M.J. Schöning, R. Thoelen, T. Wagner, Towards light-addressable flow control: Responsive hydrogels with incorporated graphene oxide as laser-driven actuator structures within microfluidic channels, Sens. Actuators B-Chem. 288 (2019) 579–585, https://doi.org/10.1016/j.snb.2019.02.086.
[12] Y. Jian, B. Wu, X. Le, Y. Liang, Y. Zhang, D. Zhang, L. Zhang, W. Lu, J. Zhang, T. Chen, Antifreezing and stretchable organohydrogels as soft actuators, Research 2019 (2019) 2384347, https://doi.org/10.34133/2019/2384347.
[13] Z. Li, P. Liu, X. Ji, J. Gong, Y. Hu, W. Wu, X. Wang, H.-Q. Peng, R.T.K. Kwok, J.W. Y. Lam, J. Lu, B.Z. Tang, Bioinspired simultaneous changes in fluorescence color, brightness, and shape of hydrogels enabled by AIEgens, Adv. Mater. 32 (2020) 1906493, https://doi.org/10.1002/adma.201906493.
[14] S.Y. Zheng, Y. Shen, F. Zhu, J. Yin, J. Qian, J. Fu, Z.L. Wu, Q. Zheng, Programmed deformations of 3D-printed tough physical hydrogels with high response speed and large output force, Adv. Funct. Mater. 28 (2018) 1803366, https://doi.org/10.1002/adfm.201803366.
[15] X. Du, H. Cui, Q. Zhao, J. Wang, H. Chen, Y. Wang, Inside-out 3D reversible ion-triggered shape-morphing hydrogels, Research 2019 (2019) 6398296, https://doi.org/10.1155/2019/6398296.
[16] X. Peng, T. Liu, Q. Zhang, C. Shang, Q.-W. Bai, H. Wang, Surface patterning of hydrogels for programmable and complex shape deformations by ion inkjet printing, Adv. Funct. Mater. 27 (2017) 1701962, https://doi.org/10.1002/adfm.201701962.
[17] H. Qin, T. Zhang, N. Li, H.P. Cong, S.-H. Yu, Anisotropic and self-healing hydrogels with multi-responsive actuating capability, Nat. Commun. 10 (2019) 2202, https://doi.org/10.1038/s41467-019-10243-8.
[18] H. Jiang, L. Fan, S. Yan, F. Li, H. Li, J. Tang, Tough and electro-responsive hydrogel actuators with bidirectional bending behavior, Nanoscale 11 (2019) 2231–2237, https://doi.org/10.1039/c8nr07863g.
[19] R. Tognato, A.R. Armiento, V. Bonfrate, R. Levato, J. Malda, M. Alini, D. Eglin, G. Giancane, T. Serra, A stimuli-resoinsive nanocomposite for 3D anisotropic cell-guidance and magnetic soft robotics, Adv. Funct. Mater. 29 (2019) 1804647, https://doi.org/10.1002/adfm.201804647.
[20] A. López-Díaz, A. Martín-Pacheco, A.M. Rodríguez, M.A. Herrero, A.S. Vázquez, E. Vázquez, Concentration gradient-based soft robotics: hydrogels out of water,

Adv. Funct. Mater. 30 (2020) 2004417, https://doi.org/10.1002/adfm.202004417.
[21] J.Q. Yu, M. Bauer, J.S. Moore, D.J. Beebe, Responsive biomimetic hydrogel valve for microfluidics, Appl. Phys. Lett. 78 (2001) 2589–2591, https://doi.org/10.1063/1.1367010.
[22] Y. Tan, D. Wang, H. Xu, Y. Yang, X.L. Wang, F. Tian, P. Xu, W. An, X. Zhao, S. Xu, Rapid recovery hydrogel actuators in air with bionic large-ranged gradient structure, ACS Appl. Mater. Interfaces 10 (2018) 40125–40131, https://doi.org/10.1021/acsami.8b13235.
[23] Z. Han, P. Wang, G. Mao, T. Yin, D. Zhong, B. Yiming, X. Hu, Z. Jia, G. Nian, S. Qu, W. Yang, A dual pH-responsive hydrogel actuator for lipophilic drug delivery, ACS Appl. Mater. Interfaces 12 (2020) 12010–12017, https://doi.org/10.1021/acsami.9b21713.
[24] M.A.C. Stuart, W.T.S. Huck, J. Genzer, M. Müller, C. Ober, M. Stamm, G. B. Sukhorukov, I. Szleifer, V.V. Tsukruk, M. Urban, F. Winnik, S. Zauscher, I. Luzinov, S. Minko, Emerging applications of stimuli-responsive polymer materials, Nat. Mater. 9 (2010) 101–113, https://doi.org/10.1038/nmat2614.
[25] Y.S. Zhang, A. Khademhosseini, Advances in engineering hydrogels, Science 356 (2017) eaaf3627, doi: 10.1126/science.aaf3627.
[26] L. Dong, A.K. Agarwal, D.J. Beebe, H. Jiang, Adaptive liquid microlenses activated by stimuli-responsive hydrogels, Nature 442 (2006) 551–554, https://doi.org/10.1038/nature05024.
[27] Z. Wang, H. Zhou, W. Chen, Q. Li, B. Yan, X. Jin, A. Ma, H. Liu, W. Zhao, Dually synergetic network hydrogels with integrated mechanical stretchability, thermal responsiveness, and electrical conductivity for strain sensors and temperature alertors, ACS Appl. Mater. Interfaces 10 (2018) 14045–14054, https://doi.org/10.1021/acsami.8b02060.
[28] Y. Qiu, Y. Tian, S. Sun, J. Hu, Y. Wang, Z. Zhang, A. Liu, H. Cheng, W. Gao, W. Zhang, H. Chai, H. Wu, Bioinspired, multifunctional dual-mode pressure sensors as electronic skin for decoding complex loading processes and human motions, Nano Energy 78 (2020), 105337, https://doi.org/10.1016/j.nanoen.2020.105337.
[29] M. Bassil, M. Ibrahim, M. El Tahchi, Artificial myscular microfibers: hydrogel with high speed tunable electroactivity, Soft Matter 7 (2011) 4833–4838, https://doi.org/10.1039/c1sm05131h.
[30] L. Hua, M. Xie, Y. Jian, B. Wu, C. Chen, C. Zhao, Multiple-responsive and amphibious hydrogel actuator based on asymmetric UCST-type volume phase transition, ACS Appl. Mater. Interfaces 11 (2019) 43641–43648, https://doi.org/10.1021/acsami.9b17159.
[31] J. Li, Q. Ma, Y. Xu, M. Yang, Q. Wu, F. Wang, P. Sun, Highly bidirectional bendable actuator engineered by LCST-UCST bilayer hydrogel with enhanced interface, ACS Appl. Mater. Interfaces 12 (2020) 55290–55298, https://doi.org/10.1021/acsami.0c17085.
[32] J. Liu, W.Z. Xu, Z.W. Kuang, P.L. Dong, Y.X. Yao, H.P. Wu, A.P. Liu, F.M. Ye, Gradient porous PNIPAM-based hydrogel actuators with rapid response and flexibly controllable deformation, J. Mater. Chem. C 8 (2020) 12092–12099, https://doi.org/10.1039/D0TC00139B.
[33] J.J. Bowen, M.A. Rose, A. Konda, S.A. Morin, Surface molding of microscale hydrogels with microactuation functionality, Angew. Chem. Int. Ed. 57 (2018) 1250–1254, https://doi.org/10.1002/anie.201710612.
[34] Z.J. Wang, C.N. Zhu, W. Hong, Z.L. Wu, Q. Zheng, Cooperative deformations of periodically patterned hydrogels, Sci. Adv. 3 (2017), e1700348, https://doi.org/10.1126/sciadv.1700348.
[35] Y.S. Kim, M. Liu, Y. Ishida, Y. Ebina, M. Osada, T. Sasaki, T. Hikima, M. Takata, T. Aida, Thermoresponsive actuation enabled by permittivity switching in an electrostatically anisotropic hydrogel, Nat. Mater. 14 (2015) 1002–1007, https://doi.org/10.1038/nmat4363.
[36] C. Ma, X. Le, X. Tang, J. He, P. Xiao, J. Zheng, H. Xiao, W. Lu, J. Zhang, Y. Huang, T. Chen, A multi-responsive anisotropic hydrogel with macroscopic 3D complex deformations, Adv. Funct. Mater. 26 (2016) 8670–8676, https://doi.org/10.1002/adfm.201603448.
[37] C. Ma, T. Li, Q. Zhao, X. Yang, J. Wu, Y. Luo, T. Xie, Supramolecular Lego assembly towards three-dimensional multi-responsive hydrogels, Adv. Mater. 26 (2014) 5665–5669, https://doi.org/10.1002/adma.201402026.
[38] L. Huang, R. Jiang, J. Wu, J. Song, H. Bai, B. Li, Q. Zhao, T. Xie, Ultrafast digital printing toward 4D shape changing materials, Adv. Mater. 29 (2017) 1605390, https://doi.org/10.1002/adma.201605390.
[39] S. Maeda, Y. Hara, T. Sakai, R. Yoshida, S. Hashimoto, Self-walking gel, Adv. Mater. 19 (2007) 3480–3484, https://doi.org/10.1002/adma.200700625.
[40] T. Li, G. Li, Y. Liang, T. Cheng, J. Dai, X. Yang, B. Liu, Z. Zeng, Z. Huang, Y. Luo, T. Xie, W. Yang, Fast-moving soft electronic fish, Sci. Adv. 3 (2017), e1602045, https://doi.org/10.1126/sciadv.1602045.
[41] S. Wei, W. Lu, X. Le, C. Ma, H. Lin, B. Wu, J. Zhang, P. Théato, T. Chen, Bioinspired synergistic fluorescence-color-switchable polymeric hydrogel actuators, Angew. Chem. Int. Ed. 58 (2019) 2–11, doi: info:doi/10.1002/ange.201908437.
[42] J. Zheng, P. Xiao, X. Le, W. Lu, P. Théato, C. Ma, B. Du, J. Zhang, Y. Huang, T. Chen, Mimosa inspired bilayer hydrogel actuator functioning in multi-environments, J. Mater. Chem. C 6 (2018) 1320–1327, https://doi.org/10.1039/C7TC04879C.
[43] W. Fan, C. Shan, H. Guo, J. Sang, R. Wang, R. Zheng, K. Sui, Z. Nie, Dual-gradient enabled ultrafast biomimetic snapping of hydrogel materials, Sci. Adv. 5 (2019) eaav7174, doi: 10.1126/sciadv.aav7174.
[44] C. Ma, W. Lu, X. Yang, J. He, X. Le, L. Wang, J. Zhang, M.J. Serpe, Y. Huang, T. Chen, Bioinspired anisotropic hydrogel actuators with on-off switchable and color-tunable fluorescence behaviors, Adv. Funct. Mater. 28 (2018) 1704568, doi:. 10.1002/adfm.201704568.
[45] T. Iijima, T. Sibaoka, Movements of $K^+$ during shutting and opening of the trap-lobs in Aldrovanda vesiculosa, Plant. Cell. Physiol. 24 (1983) 51–60, https://doi.org/10.1093/oxfordjournals.pcp.a076513.
[46] A.S. Westermeier, R. Sachse, S. Poppinga, P. Vögele, L. Adamec, T. Speck, M. Bischoff, How the carnivorous waterwheel plant (Aldrovanda vesiculosa) snaps, Proc. R. Soc. B 285 (2018) 20180012, doi: 10.1098/rspb.2018.0012.
[47] A.S. Westermeier, N. Hiss, T. Speck, S. Poppinga, Functional-morphological analyses of the delicate snap-traps of the aquatic carnivorous waterwheel plant (Aldrovanda vesiculosa) with 2D and 3D imaging techniques, Ann. Bot. 126 (2020) 1099–1107, https://doi.org/10.1093/aob/mcaa135.
[48] A. Doring, W. Birnbaum, D. Kuckling, Responsive hydrogels-structurally and dimensionally optimized smart frameworks for applications in catalysis, micro-system technology and material science, Chem. Soc. Rev. 42 (2013) 7391–7420, https://doi.org/10.1039/c3cs60031a.
[49] S.-J. Jeon, A.W. Hauser, R.C. Hayward, Shape-morphing materials from stimuli-responsive hydrogel hybrids, Acc. Chem. Res. 50 (2017) 161–169, https://doi.org/10.1021/acs.accounts.6b00570.
[50] M.A. Haq, Y. Su, D. Wang, Mechanical properties of PNIPAM based hydrogels: a review, Mater. Sci. Eng. C 70 (2017) 842–855, https://doi.org/10.1016/j.msec.2016.09.081.
[51] L. Tang, L. Wang, X. Yang, Y. Feng, Y. Li, W. Feng, Poly(N-Isopropylacrylamide)-based smart hydrogels: design, properties and applications, Prog. Mater. Sci. 115 (2021), 100702, https://doi.org/10.1016/j.pmatsci.2020.100702.
[52] Z. Yang, L. Zhu, B. Li, S. Sun, Y. Chen, Y. Yan, Y. Liu, X. Chen, Mechanical design and analysis of a crawling locomotion enabled by a laminated beam, Extrem. Mech. Lett. 8 (2016) 88–95, https://doi.org/10.1016/j.eml.2016.03.014.
[53] L. Zhu, Y. Cao, Y. Liu, Z. Yang, X. Chen, Architectures of soft robotic locomotion enabled by simple mechanical principles, Soft Matter 13 (2017) 4441–4456, https://doi.org/10.1039/c7sm00636e.
[54] K. Haraguchi, H.-J. Li, Control of the coil-to-globule transition and ultrahigh mechanical properties of PNIPA in nanocomposite hydrogels, Angew. Chem. Int. Ed. 44 (2005) 6500–6504, https://doi.org/10.1002/anie.200502004.
[55] K. Haraguchi, T. Takada, Synthesis and characteristics of nanocomposite gels prepared by in situ photopolymerization in an aqueous system, Macromolecules 43 (2010) 4294–4299, https://doi.org/10.1021/ma902693x.
[56] S. Wang, Y. Gao, A. Wei, P. Xiao, Y. Liang, W. Lu, C. Chen, C. Zhang, G. Yang, H. Yao, T. Chen, Asymmetric elastoplasticity of stacked graphene assembly actualizes programmable untethered soft robotics, Nat. Commun. 11 (2020) 4359, https://doi.org/10.1038/s41467-020-18214-0.
[57] Z.L. Wu, M. Moshe, J. Greener, H. Therien-Aubin, Z. Nie, E. Sharon, E. Kumacheva, Three-dimensional shape transformations of hydrogel sheets induced by small-scale modulation of internal stresse, Nat. Commun. 4 (2013) 1586, https://doi.org/10.1038/ncomms2549.
[58] L. Li, J. Meng, C. Hou, Q. Zhang, Y. Li, H. Yu, H. Wang, Dual-mechanism and multimotion soft actuators based on commercial plastic film, ACS Appl. Mater. Interfaces 10 (2018) 15122–15128, https://doi.org/10.1021/acsami.8b00396.
[59] G. Qu, Y. Li, Y. Yu, Y. Huang, W. Zhang, H. Zhang, Z. Liu, T. Kong, Spontaneously regenerative tough hydrogels, Angew. Chem. Int. Ed. 58 (2019) 10951–10955, https://doi.org/10.1002/anie.201904932.

**Weizhong Xu** is currently pursuing a Ph.D. degree in the Faculty of Mechanical Engineering & Automation at Zhejiang Sci-Tech University. His research interests include hydrogel-based actuator and intelligent human-machine technologies.

**Pengli Dong** is currently pursuing a master's degree in College of Science at Zhejiang Sci-Tech University. Her research interest is developing novel functional materials for intelligent actuators.

**Senpeng Lin** is currently pursuing a master's degree in College of Mechanical Engineering at Zhejiang University of Technology. His research interest is developing novel materials for intelligent actuators.

**Zhongwen Kuang** is currently pursuing a master's degree in College of Science at Zhejiang Sci-Tech University. His research interest is developing novel materials for intelligent actuators.

**Zhiqin Zhang** is currently pursuing a master's degree in College of Science at Zhejiang Sci-Tech University. His research interest is developing novel materials for intelligent actuators.

**Dr. Shunli Wang** is currently an Associate Professor in the Department of Physics at Zhejiang Sci-Tech University. His research mainly focuses on ultra-wide band gap semiconductor $Ga_2O_3$ materials and devices.

**Dr. Fangmin Ye** is currently an Associate Professor in the Department of Physics at Zhejiang Sci-Tech University. His research mainly focuses on New energy materials and devices.

**Lin Cheng** received her Bachelor of Henan University in 2017. She is currently pursuing a Ph.D. degree in the Zhejiang Sci-Tech University. Her research interests include flexible sensor and smart materials/structures.

**Prof. Huaping Wu** received his Ph.D. degree in Engineering Mechanics from the Harbin Institute of Technology in 2009 and a Bachelor's degree from the Harbin Institute of Technology in 2002. He worked as a visiting scholar at the Kyoto University in 2014 and a postdoctoral research fellow at the City University of Hong Kong in 2012. He is currently a Professor in the School of Mechanical Engineering at Zhejiang University of Technology. His research mainly focuses on the mechanics of smart materials/structures, bionic machinery and bionic manufacturing, and flexible electronics devices.

**Prof. Aiping Liu** received her Ph.D. degree in Material Science from the Harbin Institute of Technology in 2008. She worked as a postdoctoral research fellow at the Nanyang Technological University from 2009 to 2011 and a visiting scholar at the University of Texas at Austin from 2019 to 2020. She is currently a Professor in the Department of Physics at Zhejiang Sci-Tech University. Her research mainly focuses on the functional inorganic/organic material, with special emphasis on developing novel materials including graphene with sensing and actuation characteristic for wearable physical/chemical sensors and intelligent actuators.